View metadata, citation and similar papers at core.ac.uk

brought to you by CORE

provided by DigitalCommons@URI

THE UNIVERSITY OF RHODE ISLAND

University of Rhode Island
DigitalCommons@URI

Graduate School of Oceanography Faculty Publications

Graduate School of Oceanography

2005

The Dok Cold Eddy

D. A. Mitchell
University of Rhode Island

W. J. Teague

See next page for additional authors

Follow this and additional works at: https://digitalcommons.uri.edu/gsofacpubs

Citation/Publisher Attribution

Mitchell, D. A., Teague, W. J., Wimbush, M., Watts, D. R., & Sutyrin, G. G. (2005). The Dok Cold Eddy. *Journal of Physical Oceanography, 35*, 273-288. doi: 10.1175/JPO-2684.1
Available at: https://doi.org/10.1175/JPO-2684.1

This Article is brought to you for free and open access by the Graduate School of Oceanography at DigitalCommons@URI. It has been accepted for inclusion in Graduate School of Oceanography Faculty Publications by an authorized administrator of DigitalCommons@URI. For more information, please contact digitalcommons@etal.uri.edu.

Authors
D. A. Mitchell, W. J. Teague, M. Wimbush, D. R. Watts, and G. G. Sutyrin

This article is available at DigitalCommons@URI: https://digitalcommons.uri.edu/gsofacpubs/414

The Dok Cold Eddy

D. A. MITCHELL*

Graduate School of Oceanography, University of Rhode Island, Narragansett, Rhode Island

W. J. TEAGUE

Naval Research Laboratory, Stennis Space Center, Mississippi

M. WIMBUSH, D. R. WATTS, AND G. G. SUTYRIN

Graduate School of Oceanography, University of Rhode Island, Narragansett, Rhode Island

(Manuscript received 9 September 2003, in final form 30 September 2004)

ABSTRACT

Current and temperature patterns in the Ulleung Basin of the Japan/East Sea are examined using acoustic travel-time measurements from an array of pressure-gauge-equipped inverted echo sounders moored between June 1999 and July 2001. The focus here is the formation and behavior of a persistent cold eddy observed south of Dok Island, referred to as the Dok Cold Eddy (DCE), and meandering of the Subpolar Front. The DCE is typically about 60 km in diameter and originates from the pinching off of a Subpolar Front meander between Ulleung and Dok Islands. After formation, the DCE dwells southwest of Dok Island for 1–6 months before propagating westward toward Korea, where it deflects the path of the East Korean Warm Current (EKWC). Four such DCE propagation events between January and June 2000 each deflected the EKWC, and after the fourth deflection the EKWC changed paths and flowed westward along the Japanese shelf as the "Offshore Branch" from June through November 2000. Beginning in March 2001, a deep, persistent meander of the Subpolar Front developed and oscillated with a period near 60 days, resulting in the deformation and northwestward displacement of the Ulleung Eddy. Satellite-altimeter data suggest that the Ulleung Eddy may have entered the northern Japan/East Sea. The evolution of this meander is compared with thin-jet nonlinear dynamics described by the modified Korteweg–deVries equation.

1. Introduction

Currents in the Ulleung Basin (UB) of the southwestern Japan/East Sea (JES), which largely derive from the inflow through the Korea/Tsushima Strait, are thought to be dominated by a northward-flowing western boundary current known as the East Korean Warm Current (EKWC), two branches of the Tsushima Current (Nearshore and Offshore Branches), and a Subpolar Front (SF). There have been many different descriptions of the meandering currents in the UB (Suda and Hidaka 1932; Uda 1934; Naganuma 1977; Kawabe 1982; Naganuma 1985; Katoh 1994; Morimoto and Yanagi 2001). The meander patterns include both warm- and cold-water intrusions (Ichiye and Takano 1988), and warm and cold eddies are commonly observed throughout the UB (Ichiye and Takano 1988; Isoda and Saitoh 1993; An et al. 1994; Lie et al. 1995; Isoda 1996). However, cold eddies are less frequently observed than warm eddies. The formation, structure, and time evolution of the eddies are not well understood. One very significant cold cyclonic eddy is located south of Dok Island (Dok Do) throughout much of the year. This eddy is referred to as the Dok Cold Eddy (DCE) by Mitchell et al. (2004b). Although there have been a few observations of cold eddies in the Ulleung Basin mentioned in other studies (Kawabe 1982; Tanioka 1968; and Morimoto et al. 2000), they have been almost entirely ignored in analysis of UB circulation.

Eddies are known to affect the Tsushima Current and SF and hence influence the dynamics of the entire JES. Baroclinic Rossby wave theory suggests a length scale of about 100 km for eddies in the JES (Matsuyama et al. 1990). Yoon (1997) depicts the currents in

* Current affiliation: Naval Research Laboratory, Stennis Space Center, Mississippi.

Corresponding author address: Douglas A. Mitchell, Meso- and Finescale Ocean Physics, Naval Research Laboratory, Stennis Space Center, MS 39529-5004.
E-mail: dmitchell@nrlssc.navy.mil

© 2005 American Meteorological Society

the southern JES as a series of cyclonic and anticyclonic eddies bounded by the SF, EKWC, and Tsushima Current. Characteristics and spatial distributions of warm eddies in the southwestern JES are discussed by An et al. (1994) using data gathered from 1967 to 1986. Movement of the warm eddies encompassed westward, northward, and southward trajectories but often the warm eddies remained in place for several months at a time. Bottom topography, neighboring currents, and Rossby waves are thought to influence the movement of the warm eddies. According to Isoda (1994), warm eddies in the UB generated in the vicinity of the Oki Islands propagate eastward. The eastward movement is attributed to an eastward mean current flow in the southern UB.

The Ulleung Eddy is perhaps the best known and most studied eddy feature in the JES. The warm Ulleung Eddy, present most of the time, has major and minor axes of about 168 and 86 km in the zonal and meridional directions, appears to be in geostrophic balance, and is strongly constrained by the bottom topography (Lie et al. 1995). The Ulleung Eddy originates from the EKWC and forms from a southward flow that closes into anticyclonic circulation around Ulleung Island (Tanioka 1968). The Ulleung Eddy is frequently described using hydrographic data, satellite-tracked drifter data (An et al. 1994; Lie et al. 1995), and altimetric data (Morimoto et al. 2000).

Cold eddies in the UB are generally more difficult to observe, often because of lack of a strong surface signature. Ichiye and Takano (1988) observed both warm and cold eddies, with diameters ranging from 30 to 160 km, in isotherm mapping at 100 m, using data taken during May and June 1987 from the Ten-Day Marine Reports of the Japan Meteorological Agency. These eddies are hypothesized to be formed by warm- and cold-water intrusions from fronts.

Kawabe (1982) observed a cold eddy in the DCE region in February 1972 and a meandering current in February 1973. But he noted for the month of March, in the years 1973–75, that one or two cold eddies could be seen between the east coast of Korea and the Oki Islands. He theorized that the eddies may have been cut off from meanders. Cold eddies were also observed in the DCE region by Tanioka (1968) using temperature at 100 m and dynamic topography for July 1966 and March 1967.

Morimoto et al. (2000), in a study of the eddy field of the entire JES derived from satellite altimetric data, observed a cold eddy, referred to as C2, in the vicinity where the DCE is observed here. The cold eddy identified through the altimetric data analysis corresponded well with the temperature mapped at 100 m by the Japan National Fisheries Research Institute. By using monthly mean temporal fluctuations of sea surface dynamic heights from May 1995 through January 1996, the cold eddy was found to persist 4 months, from May to August, and then to disappear in September. The cold eddy appears to have moved westward, toward the Korean coast, where it may have been absorbed by the EKWC. Morimoto et al. (2000) concluded that warm and cold eddies appear periodically in the southern part of the UB and that the lifetimes of the eddies are about 1 month. However, using lag correlation analysis, they determined an eastward propagation of about 1.8 cm s^{-1}, suggesting an eastward advection by the Offshore Branch. Based on evidence presented here on propagation of the DCE and by Morimoto et al. (2000), the eastward propagation might only be associated with warm eddies in the southern UB. Westward propagation is associated with the DCE, which can have a lifetime much longer than 1 month.

There have been many surveys of temperature and salinity in the UB by Japanese and Korean investigators. Unfortunately, political boundaries often limited the coverage areas. In addition, Korean and Japanese data were sometimes not in good agreement for the same regions and sampling periods (Kawabe 1982) and therefore were difficult to combine. Unfortunately, the DCE apparently is commonly split by the political boundary between these countries' economic zones, making it more difficult to observe. The DCE is not readily observed in sea surface temperature maps since the surface temperature differential is usually small. The DCE is clearly seen in maps of geopotential height at the surface relative to 500 dbar (lower geopotential height than surrounding waters) and in vertical sections of temperature across the eddy. The DCE is also observable in sea surface height measurements obtained from satellite altimetry data.

As part of the U.S. Office of Naval Research JES program an observational program with focus on the UB was recently completed. Data were obtained from a two-dimensional array of 23 pressure-sensor–equipped inverted echo sounders (PIESs) and 11 recording current-meter (RCM) moorings (Fig. 1) deployed for 2 yr, beginning in June 1999. The current-meter mooring sites were coordinated with those of a set of four current meter moorings deployed by the Korean Ocean Research and Development Institute (KORDI) and an additional mooring deployed by the Research Institute of Applied Mechanics (RIAM) of Kyushu University. The near-bottom current data from all these moorings were used to examine the deep flow patterns and to level the PIES pressure measurements, which when combined with the PIES acoustic-echo-time data form a three-dimensional mapping of the current field (Mitchell et al. 2004, 2005). These data have been used to observe the time-varying currents and eddies, and will be used to understand the coupling between the shallow and deep currents and eddies and to quantify cross-frontal and vertical fluxes associated with mesoscale processes (Mitchell et al. 2005; Teague et al. 2005b).

This paper concentrates on the meandering of the SF

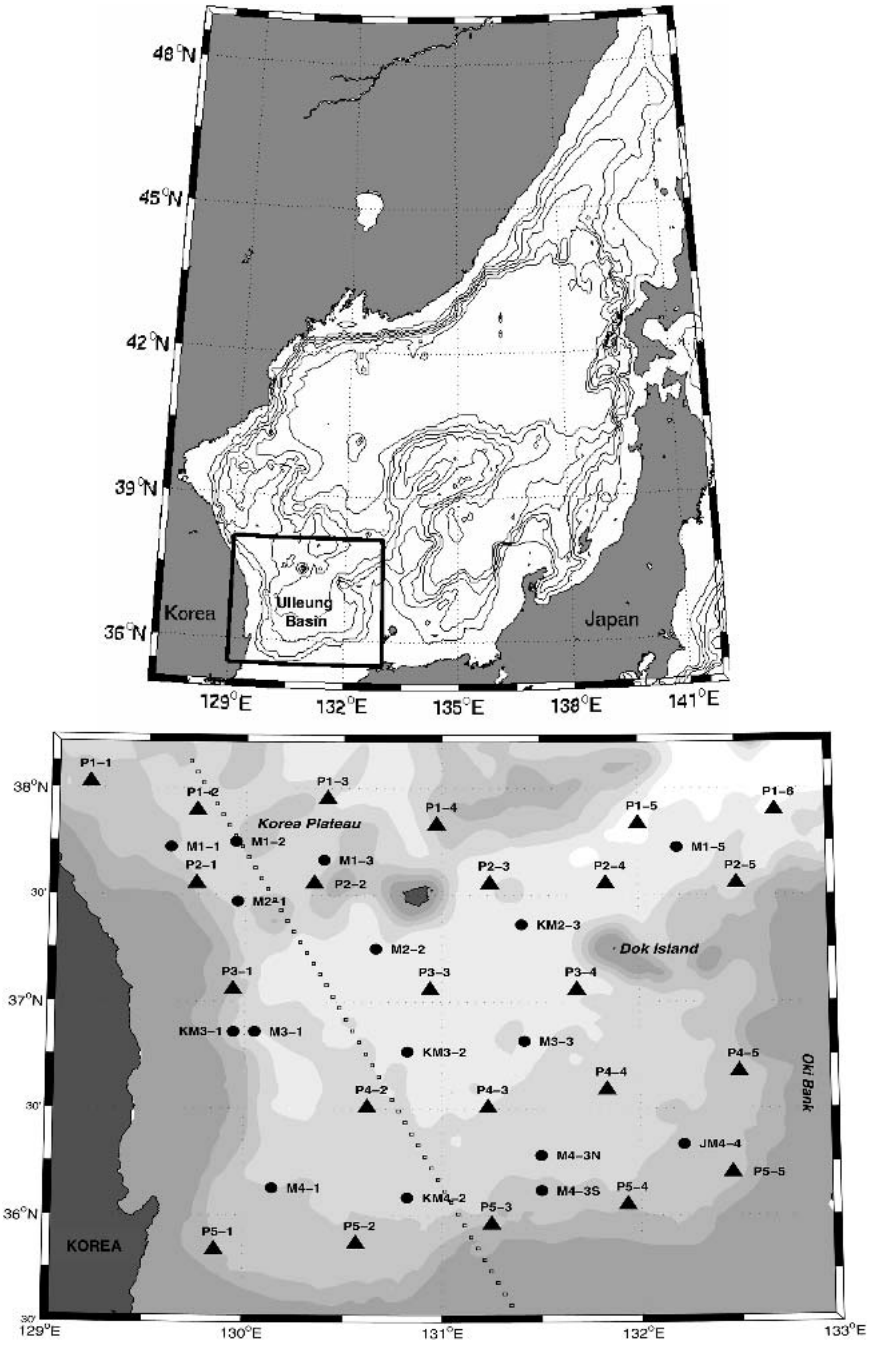

FIG. 1. (top) Topographic map of the Japan/East Sea. The heavy black box represents the study area. Contour interval is 500 m. (bottom) Topographic map of the Ulleung Basin. The locations of the PIES (black triangles) and current meters (dark circles) are shown. The ground track of TOPEX/Poseidon line 112 is marked by small open black squares. Contour interval is 500 m.

in the UB and on the DCE. A large meander of the SF, with wavelength and amplitude of about 200 km, commonly forms in the UB. The meander can persist for several months and may be described using thin-jet theory under particular conditions. The DCE most likely forms from the meander through an instability process, followed by a retreat of the meander. The DCE was typically about 60 km in diameter. Its center was commonly observed between 130.5° and 132°E during the 2-yr measurement period. The DCE can have a major impact on the circulation in the UB and therefore the entire JES.

2. Data

Twenty-five pressure-gauge-equipped inverted echo sounders were deployed during June 1999 as 5 × 5 array with 50–60-km spacing covering a 220 km × 240 km region in the UB (Fig. 1). Twenty-three of these PIESs were recovered in June–July 2001, with deep crab fishing activities probably responsible for the two losses. Instrument spacing was selected to allow coherent mapping of mesoscale features, based on a correlation length scale of 100 km estimated for upper-layer features using Rossby wave theory (Matsuyama et al. 1990).

A PIES measures vertical acoustic travel time with an accuracy 1.6 ms and a resolution of 0.05 ms, abyssal pressure with a resolution of 0.001 dbar and an accuracy of 0.1–0.3 dbar, and temperature (used to correct the Digiquartz pressure transducer's temperature sensitivity) with an accuracy of 0.15°C and a resolution of 0.0007°C. All measurements were recorded hourly. The vertical profile of temperature and specific volume anomaly can often be inferred from a travel time measurement through the gravest empirical mode (GEM) technique, originally developed by Meinen and Watts (2000). In order to improve the interpretation of PIES data and separate the eddy variability from the spatially varying seasonal signal that extends through the depth of the shallow JES thermocline, the GEM technique is enhanced by a combined analysis with the U.S. Navy's Modular Ocean Data Assimilation System (MODAS) static climatology (Fox et al. 2002), which contains the spatially variable seasonal signal. This new method, referred to as the residual GEM technique, is fully described by Mitchell et al. (2004).

3. Observations from PIES data

The surface temperature signature of the DCE, which is just a fraction of a degree, is not readily identified in sea surface temperature maps. However, the DCE is clearly identifiable at 100-m depth where the signature is often greater than 2°C. The structure of the DCE suggests that the vertical integral of specific volume anomaly, that is, geopotential height [primarily determined by temperature variations in the Ulleung Basin (Mitchell et al. 2004)], is the appropriate parameter for studying the behavior of the DCE. The residual GEM technique estimates dynamic height, defined as the geopotential height at the surface relative to 500 dbar divided by the acceleration of gravity, with a precision of 2.44 cm (Mitchell et al. 2004). The range of dynamic height in the UB is about 60 cm, giving a signal-to-noise ratio of 25:1. In addition, the use of dynamic height allows direct comparisons with satellite altimeter sea surface height measurements and their associated geostrophic currents.

The mean positions of the EKWC, Ulleung Eddy, SF, and DCE are easily discerned in a map of the average dynamic height in the UB derived from the PIES measurements (Fig. 2). The Ulleung Eddy has a mean diameter of about 135 km and is centered southwest of Ulleung Island. The mean path of SF meanders extends to the south along 131.9°E, which is approximately the longitude of Dok Island. The DCE has a mean diameter of 60 km and is centered near 131.4°N, 36.6°E when it is stationary. The path that the DCE follows while propagating westward is along the southern edge of the Ulleung Eddy at about 36.2°E, which is also the mean latitude where it crosses Ocean Topography Experiment (TOPEX)/Poseiden (T/P) satellite-altimeter line 112 (Fig. 1). Clearly, the DCE was present often enough during the 2-yr measurement period to leave a clearly defined signature in the mean dynamic height field.

Maps of dynamic height on representative days for seven different events are shown in Fig. 3. The DCE is well defined throughout much of the 2-yr measurement period, and its center, prior to westward propagation, is generally located between 36° and 37°N with an easternmost extreme location of about 132.5°E (Fig. 3, event 7) at the end of the measurement period. The DCE either remains almost stationary or tends to propagate westward toward Korea with speeds of 6–8 cm s^{-1}, which is significantly higher than the 1–2 cm s^{-1} predicted for internal Rossby waves according to $c = -\beta\lambda^2$, where c is the phase speed, β is the northward gradient of the Coriolis parameter, and λ is the internal Rossby radius (~5–10 km in UB). When stationary, it tends to elongate in the north–south direction and, when propagating, it tends to elongate in the east–west direction. Its shape and position vary with fluctuations of the Offshore Branch position, changing from nearly circular when the Offshore Branch is weak to more elliptical when the Offshore Branch is strong (Mitchell et al. 2005).

The DCE was centered near 36.6°N, 131.6°E from June through November 1999 (Mitchell et al. 2005) before propagating westward. Prior to formation of the Ulleung Eddy, from 30 June through 20 July 1999 (not shown) the transport through the Korea/Tsushima Strait diminished from 3 Sv (Sv ≡ 10^6 m^3 s^{-1}) to 2 Sv (Teague et al. 2002, 2005a). In late July 1999 the DCE began to split into two eddies, a larger eddy to the south and a smaller eddy to the north (Fig. 3, event 1). The smaller northern DCE propagated northwestward above the still-forming Ulleung Eddy and merged with the cool waters along the Korean coast near 38°N. After 20 July 1999 the inflow through the Korea/Tsushima Strait increased to a maximum of 5 Sv during which time the Ulleung Eddy increased its size (Fig. 3, event 2) in response to the increased transport. The Ulleung Eddy expanded northward and completely filled the northern UB from the Korean coast to the Oki Spur by 15 November 1999. During the Ulleung Eddy expansion, the southern DCE remained nearly stationary until December 1999 (Mitchell et al. 2005).

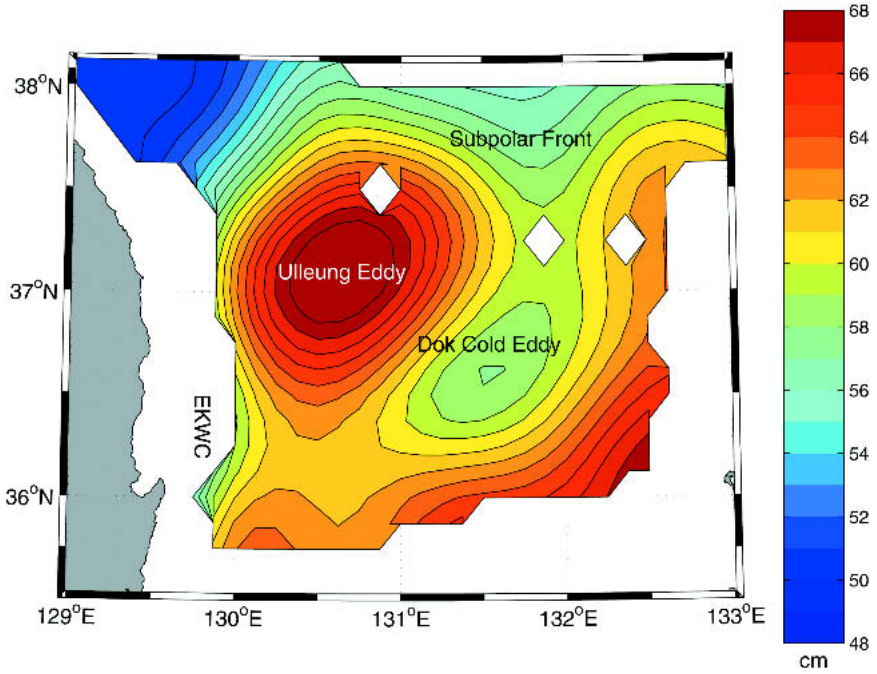

FIG. 2. Average dynamic height (geopotential height anomaly at surface relative to 500 dbar divided by the acceleration of gravity; cm) over the 2-yr deployment in the Ulleung Basin. The mean positions of the EKWC, Ulleung Eddy, Subpolar Front, and the Dok "Cold Eddy" are labeled. The white diamonds, from left to right, are Ulleung Island, Dok Island, and a seamount that reaches within 500 m of the surface.

Between December 1999 and June 2000, the DCE propagated westward and merged with the EKWC four separate times (Fig. 3, events 2–5). The first time, the DCE propagated westward toward Korea in December 1999 and was absorbed by the EKWC in late January 2000 (event 2). In early February 2000, the DCE re-formed and remained nearly stationary until it began to propagate toward Korea on about 25 March, reaching the region of the Korean coast on 6 April 2000 (event 3). Soon after, the DCE re-formed on about 18 June 2000 and immediately propagated southwestward, reaching the Korean coast in early July 2000 (event 5). During each of these four DCE propagation events, a portion of the EKWC was diverted eastward south of 36.5°N. After the first three events, the EKWC returned approximately to its prior path.

Immediately following the fourth DCE westward propagation event, the EKWC was fully diverted away from the Korean coast and followed a new path eastward along the Japanese shelf break before turning north along the Oki Spur. The flow of warm water along this path is traditionally referred to as the "Offshore Branch" (Mitchell et al. 2005). After the diversion of the EKWC into the Offshore Branch, the Ulleung Eddy divulged a significant portion of its mass to the east into the Offshore Branch (Fig. 3, event 5, 22 July 2000). Following this, an extreme deepening of a meander trough of the SF that nearly extended to the coast of Korea occurred in August 2000 (Fig. 3, event 5). Correspondingly, the warm Ulleung Eddy became isolated and entirely surrounded by cold waters.

After reestablishment of the EKWC in early November 2000, a larger DCE reformed in late November (Fig. 3, event 6) and remained fairly stationary. Steep troughs developed in the SF and twice enveloped the DCE (29 January and 10 March 2001), sometimes obscuring the DCE. The first time, the DCE merged with the meander and was reshed as the meander retreated. The second time, however, the meander trough persisted and strengthened. Figure 3 (event 7) shows the behavior of the large meander from the time of recapture of the DCE until the time our array of instruments was recovered in June 2001. During this period the amplitude of the meander is about 200 km, and the trough oscillates in the east–west direction with a period of about 60–90 days. In early June 2001, a small DCE separated from the SF meander and remained near 36.5°N, 132.5°E for the remaining duration of our measurement period. Also of note during the oscillation of the SF meander, the Ulleung Eddy narrows in the east–west direction, elongates in the north–south direction and is steadily displaced to the northwest until the entire eddy is north of Ulleung Island, the only time this occurs during our measurement period.

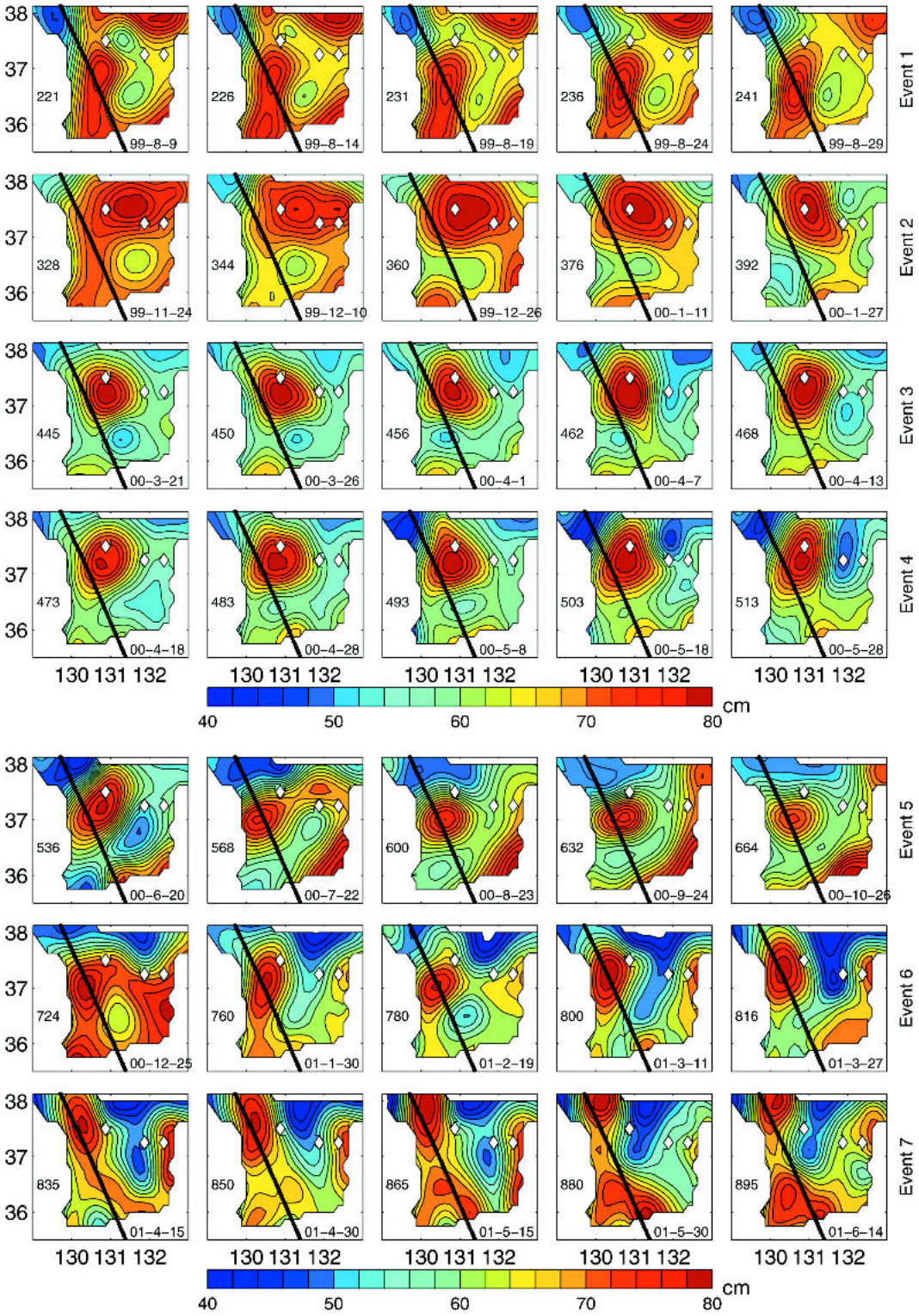

FIG. 3. Maps of dynamic height (cm) for seven events discussed in text. Event 1: DCE propagates westward north of the forming Ulleung Eddy. Events 2, 3, 4: The DCE propagates westward along 36.3°N and is absorbed by the EKWC. Event 5: The propagating DCE fully diverts the EKWC eastward into the Offshore Branch and the EKWC remains absent for 5 months. Event 6: The DCE is shed and recaptured by the SF meander twice. Event 7: The SF meander persists and oscillates with a period of about 60 days and the Ulleung Eddy gets distorted and displaced northward.

4. Observations from T/P data

Nearly a decade of T/P altimetry data from December 1992 to March 2002 is used for analysis. TOPEX/Poseiden ground track 112, oriented northwest to southeast, crosses the western half of the PIES array (Fig. 1). From these data alone, only surface geostrophic velocity anomalies normal to the line can be calculated. However, using a technique described by Teague et al. (2004), an absolute referencing of the T/P data is obtained by using the three-dimensional maps of specific volume anomaly produced from the two years of PIES data. Surface geostrophic velocities on the T/P track and normal to it can then be calculated over the entire T/P time period and are analyzed here for the time period of 1993–2002. The T/P sampling interval is approximately ten days with a spatial resolution of about 6 km.

A better understanding of the T/P data can be obtained by analyzing it in conjunction with the available PIES data along the T/P ground track (Fig. 4). The PIES data along the T/P line can be analyzed within the context of the circulation for the entire UB (Mitchell et al. 2005) and the signatures of the DCE and SF meander, within that framework, can be determined. For an ideal case of a cold eddy crossing a T/P line within a uniformly warmer ocean, the eddy's T/P signature would be a low in dynamic height with a corresponding negative velocity core at its northern edge and a positive velocity core at its southern edge. This is indeed a signature left by the DCE in the PIES and T/P data (Fig. 4, noted by the letter D). However, matters in the UB are complicated because of the complex and changing circulation patterns found in the UB (Mitchell et al. 2005), particularly by the presence of the Ulleung Eddy and the Offshore Branch. Furthermore, due to the limited spatial coverage of the PIES data and T/P data (due to contamination by land), particularly south of 36°N, the southern positive velocity core is sometimes difficult to discern clearly. Furthermore, after passage of the DCE the diverted EKWC does not immediately return to its prior path, but can remain diverted over the T/P line for several weeks to several months. Also, as seen in Fig. 3 (event 5), propagation of the DCE across the T/P line can be followed by an extended stay of cold water over the T/P line, resulting in a loss of the return to higher dynamic heights associated with the passing of the DCE. Thus, half the DCE signature in the dynamic height field may be missing. The DCE can also propagate north of 37°N when the Ulleung Eddy is not fully established (Fig. 3, event 1). The signature of the DCE crossing the T/P line, in this case, is marked by a low dynamic height notch within an otherwise northward propagating high (Fig. 4, noted by the letter H) associated with the formation of the Ulleung Eddy. The signature is less clear because the warm waters associated with the forming Ulleung Eddy and the cold waters along the coast of Korea create such a strong dynamic height gradient that the DCE is not clearly delineated from it in either height or velocity fields.

The SF meander leaves a clear signature in both the dynamic height and geostrophic velocity fields. The dynamic height signature, as seen propagating from southwest to northeast, is marked by a low dynamic height beginning near 37°N followed by a high dynamic height (Figs. 4 and 5, noted by the letter M). The low is generated by the cold water associated with the meander crossing the T/P line and the high by the warm water associated with the Ulleung Eddy. This low–high sequence typically migrates northward beyond 38°N in 2–6 months. The velocity signature, also as seen propagating from southwest to northeast, begins with a strong negative velocity beginning near 37°N followed by a strong positive velocity (Figs. 4 and 5, noted by M). The negative velocity comes from the meander crossing the T/P line on a southwestward trajectory, while the positive velocity is associated with the western edge of the Ulleung Eddy. As in the height field, this velocity sequence also migrates northward in 2–6 months.

The DCE signature can be seen in the decade of T/P data on 17 occasions (Figs. 4 and 5, noted by D or H). There are eleven occurrences (noted by a black D), February and July 1993; March 1994; July 1996; October 1998; January, April, May, July, and September 2000; and March 2001, that have clean signatures in both the dynamic height and geostrophic velocity fields, that is, a clear low in the height field along with the associated negative and positive velocity cores along its northern and southern edges. There are three occurrences (noted by a magenta D) where the signature is clearly seen in the velocity field, but the signature in the height field is obscured because the passing of the DCE is followed by a period of cold water over the T/P line. They occur in January and December 1995 and April 1997. There are four occurrences of the DCE propagating westward north of 37°N. They occur in August 1993, May and July 1997, and August 1999.

The SF meander signature can be seen in the decade of T/P data on seven occasions (Figs. 4 and 5, noted by M). They occur in December 1993–June 1994, August–November 1994, August–November 1995, September–November 1996, August–October 1997, May–July 1998, and April–August 2001. In all seven cases, the high dynamic height values associated with the Ulleung Eddy are advected steadily northward by the oscillating meander until they pass north of 38°N and out of the UB.

5. Thin-jet theory

Thin-jet models have been used with some success in the ocean in studies of meandering and eddy detachment (Robinson and Niiler 1967; Pratt 1988; Cushman-Roisin et al. 1993). In the thin-jet approximation, variations along the jet axis are assumed to be gradual in

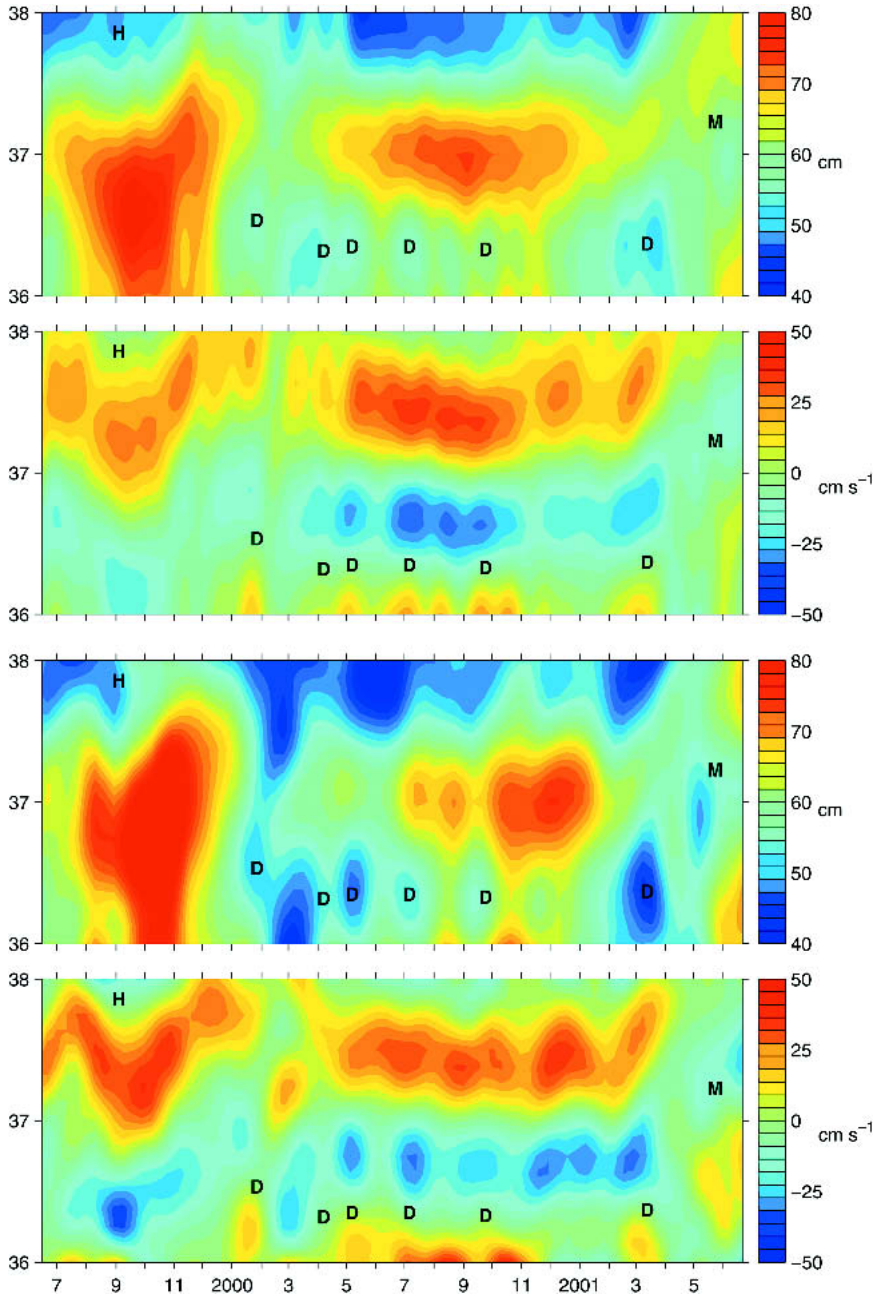

FIG. 4. (top) Dynamic height (cm) along T/P track 112 derived from the PIES data. (second) Geostrophic velocity (cm s^{-1}) along T/P track 112 derived from the PIES data. (third) T/P measured dynamic height (cm) along T/P track 112. (bottom) T/P geostrophic velocity (cm s^{-1}) along T/P track 112. DCEs and SF meanders are labeled as follows: black D, DCE; black H, DCE north of 37°N; black M, persistent SF meander.

comparison with variations normal to the axis. As a result, along- and cross-axis structures can be decoupled, allowing a semianalytic description of nonlinear meandering. This technique can be applied where eddy-forming meanders have wavelengths much longer than the across stream width.

Flierl and Robinson (1984) discuss meandering and stability problems of thin-jet dynamics and describe meandering motions using the cross-stream integrated vorticity balance. According to linear theory, under the long-wave approximation, unstable meanders occur when wavelengths are less than some critical wavelength, which is about 150 km for the Gulf Stream for example. A similar calculation for the JES renders a

critical wavelength of about 140 km. The shorter-scale unstable disturbances, which are found to have maximum growth rates and retrograde phase speeds, are not well represented because their scale is near that of the deformation radius, where the long-wave approximation breaks down. However, as discussed by Pedlosky (1981), the most rapidly growing linear wave is not always the one seen at finite amplitude. Flierl and Robinson (1984) further suggest that the observed large-scale meanders may be stable or weakly growing meanders forced by the inlet conditions, while the shorter rapidly growing instabilities either equilibrate or dissipate at small amplitudes.

Cushman-Roisin et al. (1993) investigate time-dependent meandering of thin ocean jets with a reduced-gravity, β-plane, nonquasigeostrophic model that may include outcropping of the density interface. They expand the governing equations in terms of a small parameter ϵ, which is the radius of deformation multiplied by the meander curvature, and derive the following set of equations to describe the midjet path:

$$\partial_s X \partial_t Y - \partial_s Y \partial_t X = a\partial_s K + b\partial_s Y, \tag{1}$$

$$(\partial_s X)^2 + (\partial_s Y)^2 = 1, \quad \text{and} \tag{2}$$

$$K = \partial_s X \partial_{ss}^2 Y - \partial_s Y \partial_{ss}^2 X, \tag{3}$$

where X and Y are Cartesian coordinates of the jet, s is the distance along the jet, K is the curvature, and t is the time. The coefficients a and b are defined by the cross-jet structure and the beta effect:

$$a = \frac{g'^2}{f_0^3(h_1 - h_2)} \int h(dh/dn)^2\, dn \quad \text{and} \quad b = \frac{\beta g'(h_1 + h_2)}{2f_0^2}. \tag{4}$$

Here g' is reduced gravity, f_0 is the Coriolis parameter, h_1 and h_2 are two limiting values of the layer depth far from the jet, n denotes the distance across the jet, and $\beta = df/dy$ describes the beta effect. Equation (1) indicates that the normal velocity to the jet segment is proportional to the rate of change of centrifugal force along the path ($\partial K/\partial s$) and the azimuth angle from the zonal direction ($\partial Y/\partial s$).

Introducing the local azimuth of the jet ϕ so that

$$\partial_s X = \cos\phi, \quad \partial_s Y = \sin\phi, \quad \text{and} \quad K = \partial_s \phi, \tag{5}$$

then from Eqs. (1)–(3) a single equation can be obtained:

$$\partial_t \phi = a\partial_{sss}^3 \phi + \frac{a}{2}(\partial_s \phi)^3 + c_0(t)\partial_s \phi. \tag{6}$$

The function $c_0(t)$ is determined by the boundary conditions at the inflow where $s = 0$ and $X = Y = 0$. The angle $\phi(0, t)$ and curvature $K(0, t)$ are prescribed by

$$c_0 = b\cos\phi(0, t) - \frac{a}{2}[\partial_s \phi(0, t)]^2. \tag{7}$$

For an initial value problem in an unbounded domain when a localized perturbation of the jet is considered, $c_0 = b$, and the path [Eq. (6)] can be further transformed into the modified Korteweg–deVries (mKdV) equation for the curvature. The mKdV equation is known to describe a variety of long, nonlinear waves, where the dispersive and nonlinear terms [the first and second terms in (Eq. (6)] balance. The envelope solitary wave, or "breather," is particularly interesting for interpreting the observations presented here.

The detachment of eddies from such a jet begins when different segments of the jet path come into contact, causing the initially simply connected jet to "pinch" together. This pinching process is effected primarily by breather solutions to the mKdV equation (Ralph and Pratt 1994). For a given initial condition the solution will evolve into a dispersive wave train plus a finite number of breathers, the connectivity of which is determined by a steepness parameter lambda. Using the scattering transform for the mKdV equation the value(s) of lambda can be calculated in a straightforward manner, and the detachment (or lack thereof) of meanders can be forecast to a high degree of confidence by calculating lambda. Examples with simple meander disturbances show a remarkable degree of stability and resistance to detachment.

6. Thin-jet dynamics in observations

The SF develops deep meanders between Ulleung and Dok Islands that can persist from weeks to months. Once a meander has formed, our PIES observations indicate two different processes can occur: 1) the meander can persist for a few months while oscillating in the east–west direction (Fig. 6, panels 1 and 2) or 2) the meander can pinch off, forming a DCE (Fig. 6, panels 3 and 4). There is a correlation between which process occurs and the separation angle θ, which is related to ϕ by $\theta = 90 - \phi$, of the EKWC relative to the coast of Korea. Our observations show that θ varies between 0° (when the EKWC flows northward after separation) and 90° (when the EKWC separates eastward). Ramp et al. (2005) suggest that the separation angle is given by $\theta = \arctan(N/M)$, where M and N are the depth integrated momentum transports by the EKWC and North Korean Cold Current (NKCC), respectively. When N/M is much less than 1, θ is near 0° and when this ratio is much greater than 1, θ is near 90°. When θ is near 90° the meander tends to pinch off into a DCE. When θ is near 0° the EKWC separates from the coast as a free flowing inertial jet, resulting in persistence of the SF meander for 2–6 months (as seen in the T/P data). During this period the SF behavior can be related to thin-jet theory with some caution due to possible effects of the Ulleung Eddy.

Application of thin-jet theory to the SF meander in the UB provides valuable insight into some aspects of

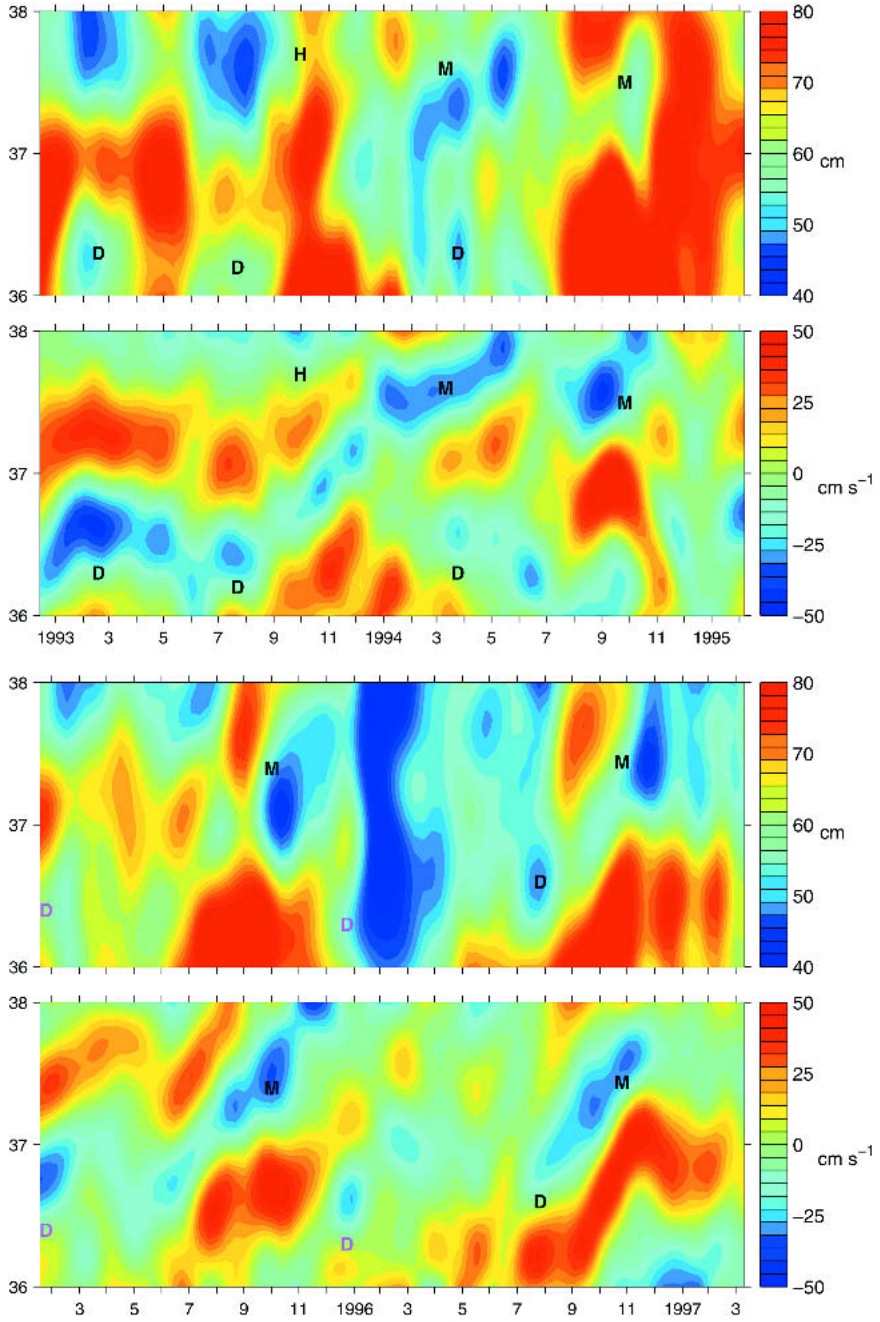

FIG. 5. (top) T/P measured dynamic height (cm) along T/P track 112 from Dec 1992 through Feb 1995, (second) T/P measured geostrophic velocity (cm s^{-1}) along T/P track 112 from Dec 1992 through Feb 1995, (third) T/P measured dynamic height (cm) for Feb 1995 through Mar 1997, (fourth) T/P measured geostrophic velocity (cm s^{-1}) from Feb 1995 through Mar 1997, (fifth) T/P measured dynamic height (cm) from Mar 1997 through May 1999, (sixth) T/P measured geostrophic velocity (cm s^{-1}) from Mar 1997 through May 1999, (seventh) T/P measured dynamic height (cm) from Jun 2001 through Mar 2002, and (eighth) T/P measured geostrophic velocity (cm s^{-1}) from Jun 2001 through Mar 2002. DCEs and the SF meander are labeled as follows: black D, DCE; magenta D, a DCE followed by cold water; black H, DCE north of 37°N; black M, persistent SF meander.

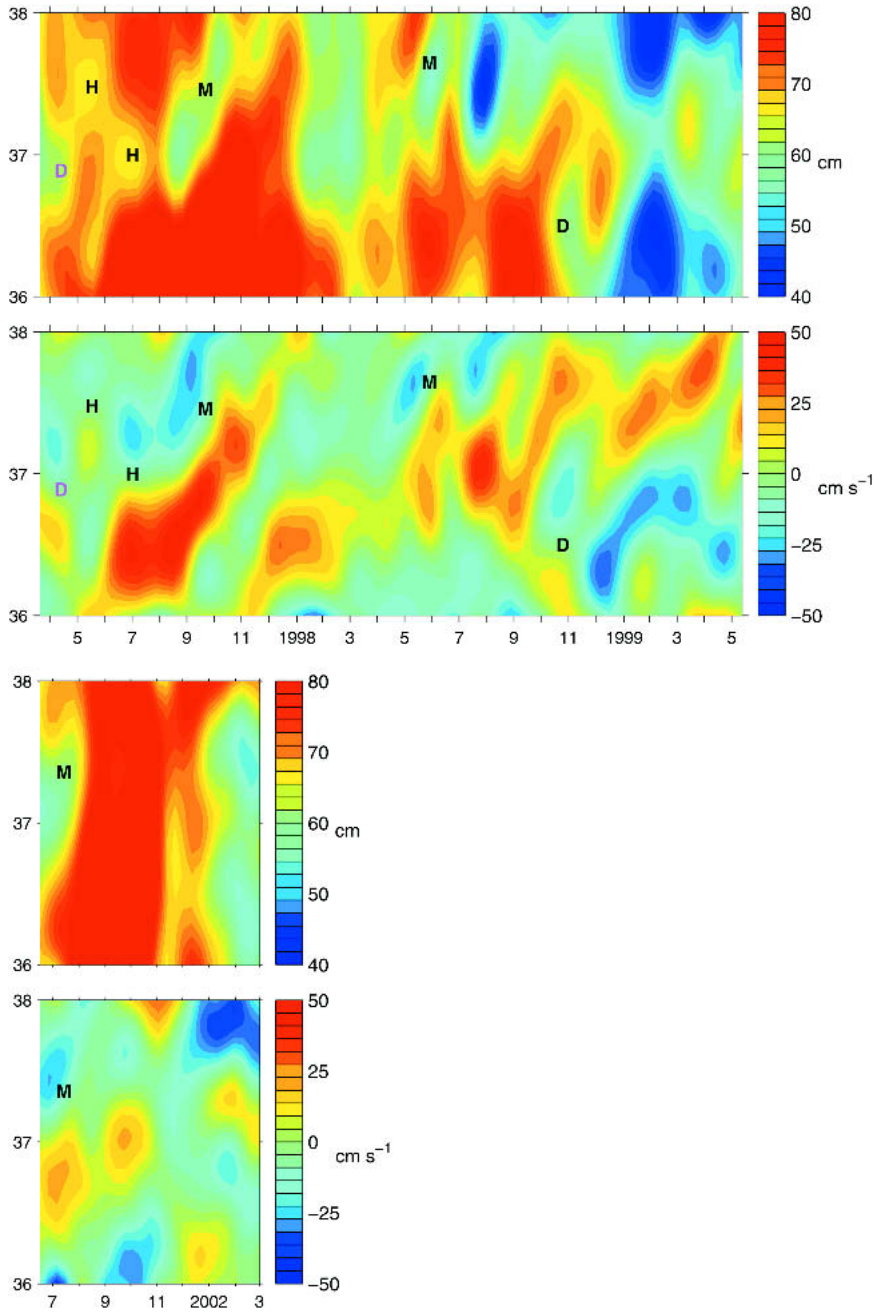

FIG. 5. (*Continued*)

the complex behavior of the SF. The observed SF meanders in the UB have a wavelength (λ_w; Fig. 6, panel 1) of about 225 km. The wavelength of the meander appears to be constrained by Ulleung Island (approximate mean position of the northern edge of the Ulleung Eddy; Fig. 2) and the Oki Spur. The critical meander scale L (Cushman-Roisin et al. 1993), which is the length scale where planetary vorticity changes and meander curvature effects balance each other in the rhs of Eq. (1) and the meander remains stationary, is given by $L = \sqrt{a/b}$. In the UB, L ~235 km for R_d = 10 km, Coriolis $f_0 = 0.877 \times 10^{-4}$ s^{-1}, and its northward gradient $\beta = 1.83 \times 10^{-11}$ m^{-1} s^{-1}, giving a critical meander scale approximately equal to the observed SF meander wavelength. Therefore, such a meander may remain stationary in the UB until interactions between the cross-jet structure with the curvature and β terms balance. The southern edge of the meander trough is typically adjacent to water cooler than the southern edge of the meander crest, which is immediately adja-

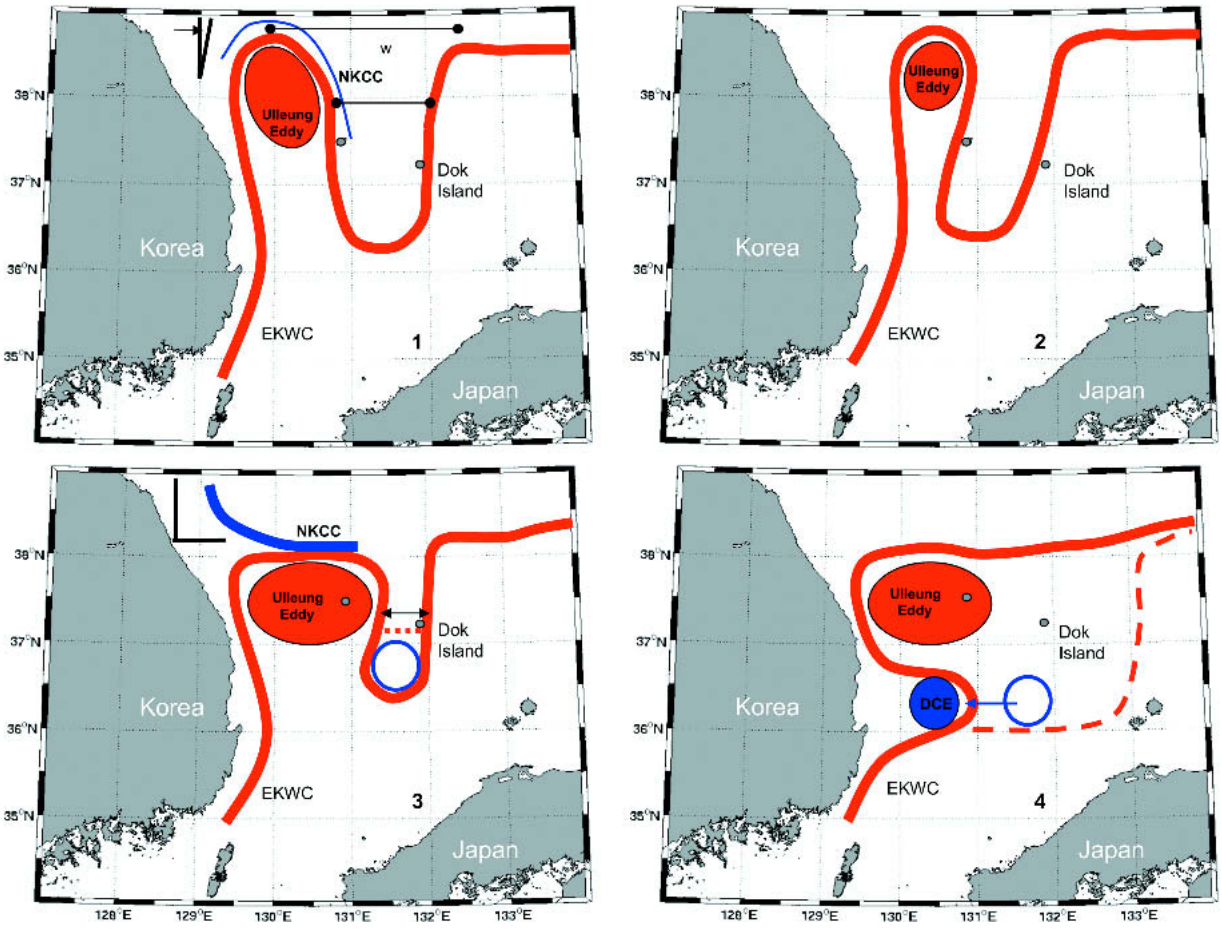

FIG. 6. (top) Schematic representation of the meandering SF meander: θ represents the separation angle of the EKWC relative to the coast of Korea, λ_w is the meander wavelength, and λ is the meander width. The thin blue line represents a weak NKCC, relative to the EKWC. (bottom) Schematic representation of the shedding of a DCE and its effect on the EKWC when it propagates westward. (left) Theta represents the separation angle of the EKWC relative to the coast of Korea, and λ is the meander width. The heavy blue line represents a strong NKCC, relative to the EKWC, forcing it to separate at a high angle. The open blue circle represents the DCE waiting to be shed. The heavy dashed red line shows where the meander will pinch off. (right) The thin blue line represents where the DCE was stationary. The thick blue vector shows its propagation path. The solid blue circle shows the DCE diverting the EKWC. The thick dashed red line represents the possibility that the DCE can fully divert the DCE into the Offshore Branch.

cent to the warm Ulleung Eddy (Fig. 3, event 7). Under these conditions the cross-jet temperature gradient in the trough is significantly less than that of the crest and results in a reduction in magnitude of the curvature term in the trough. When the meander is not growing, as is the case here, the result is a reduction of the β term, which is proportional to the azimuth angle of the jet from the zonal direction. Thus, the bottom of the trough flattens, as seen in Fig. 3, event 7.

Breather solutions to the mKdV equation are packets of waves propagating through an envelope of permanent form. The propagating waves cause the envelope to oscillate so that a large amplitude meander of one sign may evolve into a meander of opposite sign and back (see Figs. 6–8 in Cushman-Roisin et al. 1993). This kind of nonlinear breatherlike evolution can be related to the formation of the meander (Fig. 3, event 6), when the latitudinal extent of the Ulleung Eddy increases from about 125 to 200 km after which the SF meander shape begins oscillating for a few months. The excitation source for the waves passing through the meander is not known: however, a likely source may be fluctuations in the inflow through the Korea/Tsushima Strait, which is known to fluctuate strongly on time scales of weeks to months (Kim et al. 2004). In our case, the observed envelope scale is about 225 km. Assuming the waves passing through the envelope have a wavelength between 200 and 300 km, the period of oscillation can be related to the equation $T = \pi/[\gamma\alpha(\alpha^2+\beta^2)]$ of Nycander et al. (1993), where T is the oscillation period, β is the inverse length of the envelope, α is the wavenumber of the waves passing through the envelope, and γ is given by $(c_+^3 - c_-^3)/(6f_0^2)$, where c_+ and c_- are the internal gravity wave speeds on either side of

the front, resulting in T that ranges from 30 to 100 days. Figure 7 shows the development and oscillation of the SF meander. In early March 2001 θ is nearly 90° and the width of the meander (λ) is narrow, indicating the DCE may form. However, by the end of March, θ approaches zero and remains steady for the remainder of the measurement period and λ approximately doubles, after which the meander begins oscillating. Interestingly, on 14 May 2001 the meander develops a perturbation that results in the separation of a small DCE in early June (Fig. 3, event 7). The observed period of oscillation is 60–90 days, suggesting that the deformation of the Ulleung Eddy during meander formation may generate the waves passing through the envelope. Also worth noting, nearly stationary breather solutions give rise to a series of eastward propagating disturbances that may themselves become breather solutions downstream (see Pratt 1988, his Fig. 9). This indicates that significant meander activity downstream from the UB may result from formation of a large SF meander in the UB.

The separation angle of the EKWC controls which of the above processes occur by affecting the SF meander width (λ) (Fig. 6, panels 1 and 2). When θ is near 0° the west side of the meander tends to flow south near 131°E (Fig. 3, event 7) and λ remains large. In contrast, when θ is near 90° (Fig. 3, event 3) the west side of the meander flows south to the east of 131°E, causing λ to decrease. Of course, when the self-interaction of the jet occurs during the DCE formation, the thin-jet approximation is violated, and a more general model should be used. A small enough width of a large amplitude cyclonic meander is a necessary condition for an eddy to pinch off as demonstrated in reduced-gravity intermediate model simulations (Sutyrin and Yushina 1989). The DCE, once formed, may remain nearly stationary for time periods of less than a month to 6 months or more. During our measurement period, the DCE occasionally disappeared in two different ways. Sometimes the DCE propagated westward toward Korea where it merged with the EKWC (Fig. 3, events 2–5). The DCE also disappeared when the SF intruded southward, engulfing the DCE in the meander (Fig. 3, event 6). The first time the meander engulfed the DCE, the DCE was subsequently shed again as the meander pinched off. The second time the meander persisted until the end of

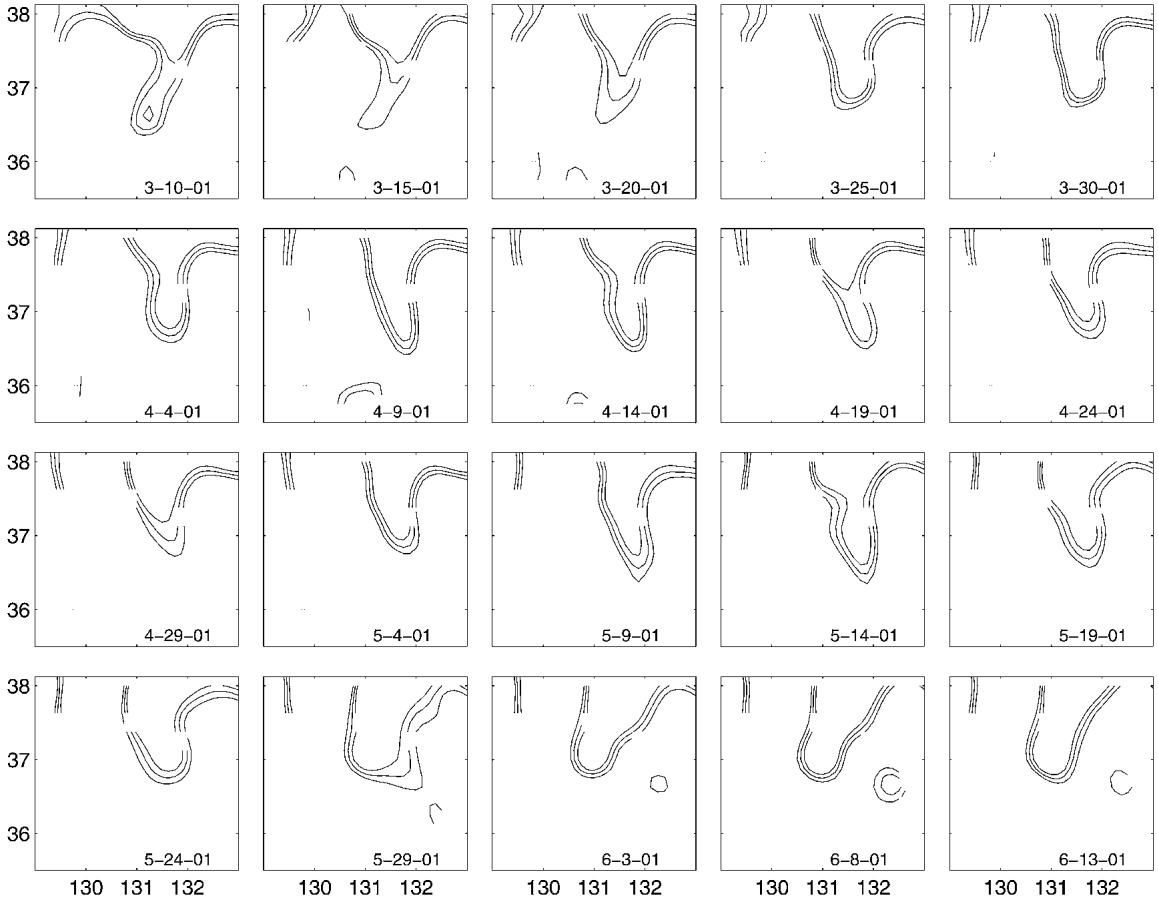

FIG. 7. Dynamic height contours (45, 47.5, and 50 cm) plotted every 4 days from 10 Mar 2001 through 13 Jun 2001, showing an oscillatory, meandering trough of the Subpolar Front.

our measurement period. As described above, the manner in which the DCE disappears is determined by θ. When the DCE approaches the coast of Korea during westward propagation the EKWC diverts eastward around it (Fig. 3, event 2, e.g.). After three such events between January and May 2000, the EKWC returned approximately to its prior path. However, after a fourth occurrence in June 2000 (Fig. 3, event 5), the EKWC was completely absent from 11 June until 5 November 2000, having been diverted into the Offshore Branch (Mitchell et al. 2005). This suggests that the DCE plays a crucial role in the rearrangement of the EKWC.

7. Seasonality

Cho and Kim (2000) and Isobe (1997) studied the branching mechanism of the Tsushima Current in the Korea/Tsushima Straits using two-layer numerical models. Cho and Kim concluded that the causal mechanism of the EKWC was the generation of negative relative vorticity through shrinkage of the upper layer caused by the intrusion of bottom cold water into the Korea/Tsushima Strait in summer. They also argued that the EKWC weakened or disappeared completely in winter when the bottom cold water retreated and could no longer cause shrinkage of the upper layer. Isobe (1997) came to a similar conclusion. A significant weakness of both these modeling studies was the northern boundary condition, which was set to allow no volume transport across the SF. Thus, external forcing, such as the presence of the DCE, was not considered. Both studies also compared their results to temperature observations, but the observations only covered a limited region (west of 131.25°E) and were collected only every two months. Thus, they were unlikely to measure a DCE because the DCE, according to our observations, resides west of 131°E only for limited durations while propagating westward. However, Isobe's Fig. 4 clearly shows the western edge of the DCE at 36.25°N, 131°E in August 1985, similar to what we observe in January 2000 [Fig. 3, event 2 (panel 5)], indicating that the event observed in August 1983 was likely the tail end of a DCE propagation after it merged with the EKWC.

The seasonality of the EKWC suggested by Cho and Kim (2000) and Isobe (1997) is present during our measurements, but was much stronger during the first year. The transport through the Korea/Tsushima Strait rose to a maximum in October 1999, fell to a minimum in January 2000, and rose to an intermediate value that remained relatively constant throughout the remainder of the PIES measurement period (Kim et al. 2004). In response to the maximum transport in October 1999, the Ulleung Eddy increased dramatically in size (Fig. 3, event 2). After the transport reached its minimum value in January 2000, the DCE became very active from January to June 2000, with four DCE propagation events. During the DCE propagation events, the EKWC was diverted eastward into the position of the Offshore Branch (Mitchell et al. 2005), temporarily resulting in a significantly weakened EKWC (Fig. 3, event 3). The EKWC again strengthened in late November 2000, but the Ulleung Eddy only slightly expanded in size (Fig. 3, event 6). After this, the DCE formed, but instead of propagating westward, it was reabsorbed by the SF meander, which persisted for the rest of our measurement period (Fig. 3, event 7). Since the transport for the second year of measurements was relatively steady and the EKWC seasonal response less pronounced than that of the first year, the seasonality of the transport must have two components: 1) variations in transport through the Korea/Tsushima Strait and 2) seasonality of the density of the inflow. This seems to agree with Cho and Kim's and Isobe's conclusions about the seasonality of the transport of the EKWC being dependent upon the increased stratification caused by the inflow of warmer waters in the summer and decreased stratification by the inflow of cooler waters in the winter. However, their conclusions are incomplete.

In stark contrast to Cho and Kim (2000) and Isobe (1997), we found the EKWC absent in summer (June–November 2000) when they argued it should be strongest due to the southward intrusion of cold bottom water under the increased temperature of the inflowing waters. Our observations indicate that the inflowing water is indeed much warmer in June 2000 (>21°C) than in February 2000 (<14°C). However, the upper surface of the bottom cold water in the presence of the impinging DCE in June 2000 rose to within 30 m of the surface, not 100 m as found by Cho and Kim (2000). This suggests that, if the bottom layer becomes too thick, the EKWC cannot flow over it, so the surface layers are not compressed. Therefore, the need to generate negative vorticity is removed and the inflowing warm waters flow east as the Offshore Branch instead of north as the EKWC. Furthermore, the disappearance and reestablishment of the EKWC does not appear to be associated with transport variations as indicated by the nearly steady transport between February 2000 and June 2001.

8. Discussion

In each of the DCE propagation events described above, the merging of the DCE with the EKWC may have resulted in the formation of a new DCE 5–10 days later. It is possible that the merging of the DCE with the EKWC, or interaction between the DCE and the Ulleung Eddy, causes a flow disturbance that grows into a meander and then develops into a new DCE; hence this is a cyclic phenomenon. The distance the disturbance travels, from the location where the DCE merges with the EKWC to where the new DCE is

formed, ranges from 250 to 300 km. The typical advection rate of the EKWC is between 0.4 and 0.6 m s^{-1}, suggesting a delay ranging from 5 to 10 days. Figure 3 (event 3) shows an interaction of the DCE with the Ulleung Eddy, which appears to initiate a disturbance on the fringe of the Ulleung Eddy that then propagates around the Ulleung Eddy, possibly initiating the next pinching off of the SF meander into a new DCE.

The disappearance of the Ulleung Eddy may be related to meandering of the SF. The PIES data indicate that, when θ is near 0°, the oscillating SF meander (Fig. 3, event 7) causes the Ulleung Eddy to narrow in the east–west direction and to lengthen and be displaced northward until the Ulleung Eddy is either no longer a coherent feature or has entered the northern JES as a warm-core eddy. The T/P data (bottom two panels, and Fig. 5, panels 7 and 8) suggest that the Ulleung Eddy left the UB and entered the northern JES, only to be replaced by a new Ulleung Eddy when the summer transport increase occurred, in a manner similar to that shown in Fig. 3 (event 1). Thin-jet theory, although it fails once the meander has oscillated far enough to impact itself, suggests that this is one of the mechanisms by which eddies can detach. The PIES data indicate that the SF meander may oscillate far enough east to impact the EKWC (Fig. 3, event 7), which would then allow the Ulleung Eddy to detach and enter the northern JES.

A low separation angle does not guarantee that a SF meander will persist. The size of the Ulleung Eddy can be increased by high transport through the Korea/Tsushima Strait (Fig. 3, events 1 and 2). A tongue of low dynamic height, stretching southward between Ulleung and Dok Islands (Fig. 3, event 1 on 29 August 1999) after the DCE propagates westward to the north of the forming Ulleung Eddy, could be interpreted as a SF meander. Soon after, the transport through the Korea/Tsushima Straits significantly increases (Teague et al. 2002), causing a significant increase in Ulleung Eddy size (Fig. 3, event 2). The expansion of the Ulleung Eddy forces the meander neck to narrow until the DCE is again pinched off from the meander. Thus, significant transport increases in summer, when the density contrast with the cold waters is highest, can cause the Ulleung Eddy to increase in size enough to pinch off the DCE despite the near-zero value of θ, which is a condition that indicates a meander may persist.

Upwelling along the southeastern coast of Korea has been frequently observed during the summer months (Byun 1989). Many different explanations have been proposed to explain this phenomenon. The classical wind-driven scenario predicts upwelling associated with southerly winds and several studies have confirmed this (Lee 1983; Lee and Na 1985; Byun 1989). Kim and Kim (1983) suggested it originated from the southward flowing NKCC, and Seung (1974) suggested that the strengthening of the EKWC during summer forced deep cold water to shoal toward the coast. One weakness of previous observations stems from their limited temporal coverage, with typical conductivity–temperature–depth (CTD) surveys taken only every two months (An et al. 1994). The results presented here (Fig. 3) clearly demonstrate that mesoscale eddy activity near the coast of Korea can occur on shorter time scales. Furthermore, our results show that structures observed north of 36°N interpreted as upwelling events based on a single CTD survey may occur as a result of the DCE propagating westward and encountering the coast of Korea. For example, Fig. 3 events 2–5 all have low dynamic height (cool) features extending out from the coast of Korea. Any of these features viewed in isolation could be interpreted as large upwelling features. However, our time series clearly shows that the westward propagation of the DCE generated these features, not upwelling.

9. Conclusions

New insight into the circulation of the UB has been gained by examining SF meanders and the previously unrecognized DCE. Large amplitude meanders (~200 km) of the SF form between Ulleung and Dok Islands. When the separation angle of the EKWC relative to Korea is near zero and the transport through the Korea/Tsushima Strait is steady, the meander oscillates in the east–west direction with a period near 60 days. Under these conditions, the dynamics of the oscillating meander can be related to a breather solution of the mKdV equation. The oscillating meander deforms and displaces the Ulleung Eddy and may result in the Ulleung Eddy being pinched off as a warm-core eddy in the northern JES.

The DCE forms when a large amplitude SF meander pinches off between Ulleung and Dok Islands. The pinching off of the DCE may occur when different segments of the jet path come into contact, causing the initially simply connected jet to "pinch" together. This pinching process is affected primarily by the width of the SF meander, which decreases when the separation angle of the EKWC increases. The DCE, once formed, may either remain stationary for many months or propagate westward toward Korea. When the DCE approaches Korea, it diverts the EKWC eastward and temporarily enhances the Offshore Branch. After the DCE has passed, the EKWC may either return to its prior path or the EKWC may remain as the Offshore Branch for an extended period, as it did between June and November 2000. Although the DCE and SF meanders have been sporadically observed in previous studies, their significance in the circulation of the UB has not been previously recognized.

Acknowledgments. This work was supported by the Office of Naval Research "Japan/East Sea DRI." Basic Research Programs include the Japan/East Sea initia-

tive under Grant N000149810246 and the Naval Research Laboratory's "Linkages of Asian Marginal Seas" under Program Element 0601153N.

REFERENCES

An, H. S., K.-S. Shim, and H.-R. Shim, 1994: On the warm eddies in the southwestern part of the East Sea (the Japan Sea). *J. Oceanol. Soc. Korea,* **29,** 152–163.

Byun, S.-K., 1989: Sea surface cold water near southeastern coast of Korea: Wind effect. *J. Oceanol. Soc. Korea,* **24,** 121–131.

Cho, Y.-K., and K. Kim, 2000: Branching mechanism of the Tsushima Current in the Korea Strait. *J. Phys. Oceanogr.,* **30,** 2788–2797.

Cushman-Roisin, B., L. Pratt, and E. Ralph, 1993: A general theory for equivalent barotropic thin jets. *J. Phys. Oceanogr.,* **23,** 91–103.

Flierl, G. R., and A. R. Robinson, 1984: On the time-dependent meandering of a thin-jet. *J. Phys. Oceanogr.,* **14,** 412–423.

Fox, D. N., W. J. Teague, C. N. Barron, M. R. Carnes, and C. M. Lee, 2002: The Modular Ocean Data Assimilation System (MODAS). *J. Atmos. Oceanic Technol.,* **19,** 240–252.

Ichiye, T., and K. Takano, 1988: Mesoscale eddies in the Sea of Japan. *La Mer,* **26,** 69–79.

Isobe, A., 1997: The determination of the transport distribution of the Tsushima Warm Current around the Korea/Tsushima Straits. *Cont. Shelf Res.,* **17,** 319–336.

Isoda, Y., 1994: Warm eddy movements in the eastern Japan Sea. *J. Oceanogr.,* **50,** 1–15.

——, 1996: Interaction of a warm eddy with the coastal current at the eastern boundary area in the Tsushima Current region. *Cont. Shelf Res.,* **16,** 1149–1163.

——, and S.-I. Saitoh, 1993: The northward intruding eddy along the east coast of Korea. *J. Oceanogr.,* **49,** 443–458.

Katoh, O., 1994: Structure of the Tsushima Current in the southwestern Japan Sea. *J. Oceanogr.,* **50,** 317–338.

Kawabe, M., 1982: Branching of the Tsushima Current in the Japan Sea. Part I: Data analysis. *J. Oceanogr. Soc. Japan,* **38,** 95–107.

Kim, C. H., and K. Kim, 1983: Characteristics and origin of the cold water mass along the east coast of Korea. *J. Oceanol. Soc. Korea,* **18,** 73–83.

Kim, K., S. J. Lyu, Y.-G. Kim, B. H. Choi, K. Taira, H. T. Perkins, W. J. Teague, and J. W. Book, 2004: Monitoring volume transport through measurement of cable voltage across the Korea Strait. *J. Atmos. Oceanic Technol.,* **21,** 671–682.

Lee, J. C., 1983: Variation of sea level and sea surface temperature associated with wind-induced upwelling in the southeast coast of Korea in summer. *J. Oceanol. Soc. Korea,* **18,** 149–160.

——, and J. Y. Na, 1985: Structure of upwelling off the southeast coast of Korea. *J. Oceanol. Soc. Korea,* **20,** 6–19.

Lie, H.-J., S.-K. Byun, I. Bang, and C.-H. Cho, 1995: Physical structure of eddies in the southwestern East Sea. *J. Korean Soc. Oceanogr.,* **30,** 170–183.

Matsuyama, M., Y. Kurita, T. Senjyu, Y. Koike, and T. Hayashi, 1990: The warm eddy observed east of Oki Islands in the Japan Sea. *Umi Sora,* **66,** 67–75.

Meinen, C. S., and D. R. Watts, 2000: Vertical structure and transport on a transect across the North Atlantic Current near 42°N: Timeseries and mean. *J. Geophys. Res.,* **105,** 21 869–21 891.

Mitchell, D. A., M. Wimbush, D. R. Watts, and W. J. Teague, 2004: The residual GEM technique and its application to the southwestern Japan/East Sea. *J. Atmos. Oceanic Technol.,* **21,** 1895–1909.

——, D. R. Watts, M. Wimbush, K. L. Tracey, W. J. Teague, J. W. Book, M.-S. Suk, and J.-H. Yoon, 2005: Upper circulation patterns in the Ulleung Basin. *Deep-Sea Res.,* in press.

Morimoto, A., and T. Yanagi, 2001: Variability of sea surface circulation in the Japan Sea. *J. Oceanogr.,* **57,** 1–13.

——, ——, and A. Kaneko, 2000: Eddy field in the Japan Sea derived from satellite altimetric data. *J. Oceanogr.,* **56,** 449–462.

Naganuma, K., 1977: The oceanographic fluctuations in the Japan Sea (in Japanese). *Kaiyo Kagaku,* **9,** 137–141.

——, 1985: Fishing and oceanographic conditions in the Japan Sea (in Japanese). *Umi Sora,* **60,** 89–103.

Nycander, J., D. G. Dritschel, and G. G. Sutyrin, 1993: The dynamics of long frontal waves in the shallow water equations. *Phys. Fluids,* **A5,** 1089–1091.

Pedlosky, J., 1981: The nonlinear dynamics of baroclinic wave ensembles. *J. Fluid Mech.,* **102,** 169–209.

Pratt, L. J., 1988: Meandering and eddy detachment according to a simple (looking) path equation. *J. Phys. Oceanogr.,* **18,** 1627–1640.

Ralph, E. A., and L. Pratt, 1994: Predicting eddy detachment for an equivalent barotropic thin jet. *J. Nonlinear Sci.,* **4,** 355–374.

Ramp, S. R., F. L. Barr, C. J. Ashjian, and L. D. Talley, 2005: The upper-ocean circulation in the Ulleung Basin during June–July 1999. *Deep-Sea Res.,* in press.

Robinson, A. R., and P. P. Niiler, 1967: The theory of free inertial jets. Part I: Path and structure. *Tellus,* **19,** 269–291.

Seung, Y.-H., 1974: A dynamic consideration on the temperature distribution in the east coast of Korea. *J. Oceanol. Soc. Korea,* **9,** 52–58.

Suda, K., and K. Hidaka, 1932: The results of the oceanographical observations aboard R.M.S. Syunpu Maru in the southern part of the Sea of Japan in the summer of 1929 (in Japanese). *J. Oceanogr. Imp. Mar. Obs.,* **3,** 291–375.

Sutyrin, G. G., and I. G. Yushina, 1989: Numerical modeling of the formation, evolution, interaction and decay of isolated vortices. *Mesoscale/Synoptic Coherent Structures in Geophysical Turbulence*, J. C. J. Nihoul and B. M. Jamart, Eds., Elsevier, **50,** 721–736.

Tanioka, K., 1968: On the East Korean Warm Current (Tosen Warm Current). *Oceanogr. Mag.,* **20,** 31–38.

Teague, W. J., G. A. Jacobs, H. T. Perkins, J. W. Book, K.-I. Chang, and M.-S. Suk, 2002: Low frequency current observations in the Korea Strait. *J. Phys. Oceanogr.,* **32,** 1621–1641.

——, ——, D. A. Mitchell, M. Wimbush, and D. R. Watts, 2004: Decadal current variations in the southwestern Japan/East Sea. *J. Oceanogr.,* **60,** 1023–1033.

——, P. A. Hwang, G. A. Jacobs, J. W. Book, and H. T. Perkins, 2005a: Transport variability across the Korea/Tsushima Strait and the Tsushima Island wake. *Deep-Sea Res.,* in press.

——, and Coauthors, 2005b: Observed deep circulation in the Ulleung Basin. *Deep-Sea Res.,* in press.

Uda, M., 1934: The results of simultaneous oceanographical investigations in the Japan Sea and its adjacent waters in May and June, 1932 (in Japanese). *Japan Imp. Fish. Exp. Sta.,* **5,** 57–190.

Yoon, J.-H., 1997: Trend of oceanography in the Japan Sea (in Japanese). *Bull. Japan. Soc. Fish. Oceanogr.,* **61,** 300–303.